THE JOURNAL OF PHYSICAL CHEMISTRY B

Article

pubs.acs.org/JPCB

Proton Transfer in Ionic and Neutral Reverse Micelles

Christian Lawler and Michael D. Fayer*

Department of Chemistry, Stanford University, Stanford, California 94305, United States

ABSTRACT: Proton-transfer kinetics in both ionic and neutral reverse micelles were studied by time-correlated single-photon counting investigations of the fluorescent photoacid 8-hydroxypyrene-1,3,6-trisulfonate (HPTS). Orientational dynamics of dissolved probe molecules in the water pools of the reverse micelles were also investigated by time-dependent fluorescence anisotropy measurements of MPTS, the methoxy derivative of HPTS. These experiments were compared to the same experiments in bulk water. It was found that in ionic reverse micelles (surfactant Aerosol OT, AOT), orientational motion (fluorescence anisotropy decay) of MPTS was relatively unhindered, consistent with MPTS being located in the water core of the reverse micelle away from the water−surfactant interface. In nonionic reverse micelles (surfactant Igepal CO-520, Igepal), however, orientational anisotropy displayed a slow multiexponential decay consistent with wobbling-in-a-cone behavior, indicating MPTS is located at the water−surfactant interface. HPTS proton transfer in ionic reverse micelles followed kinetics qualitatively like those in bulk water, albeit slower, with the long-time power law time dependence associated with recombination of the proton with the dissociated photoacid, suggesting a modified diffusion-controlled process. However, the power law exponents in the ionic reverse micelles are smaller (~ -0.55) than that in bulk water (-1.1). In neutral reverse micelles, proton-transfer kinetics did not show discernible power law behavior and were best represented by a two-component model with one relatively waterlike population and a population with a faster fluorescence lifetime and negligible proton transfer. We explain the Igepal results on the basis of close association between the probe and the neutral water−surfactant interface, with the probe experiencing a distribution of more and less waterlike environments. In addition, the observation in bulk water of a power law $t^{-1.1}$ for diffusion-controlled recombination is in contrast to the theoretical prediction of $t^{-1.5}$ and previously reported observations. The difference from prior experimental results is discussed.

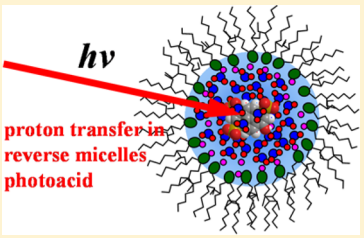

I. INTRODUCTION

Aqueous proton transfer is important in a wide variety of chemical and biological systems, and the effect of confined environments on proton transfer is relevant to many important topics, including the function of biological cells, membranes, and hydrogen fuel cells. Reverse micelles (RMs), consisting of aggregated surfactant molecules encapsulating a core water pool within a hydrophobic organic phase, provide simple and experimentally accessible systems for studying confined aqueous environments. Considerable attention has been paid to orientational dynamics, proton transfer, and other properties of water and of dissolved probes in the interior of reverse micelles.[1−7]

The fluorescent photoacid 8-hydroxypyrene-1,3,6-trisulfonate (HPTS), shown in Figure 1A, has been used for examining proton-transfer processes and the effect of differing solvent environments on proton transfer.[3,4,6,8−11] The ground-state pK_a of HPTS is 7.7, while its pK_a in its first electronic excited state is ~0.5.[12] This makes it an excellent probe for time-resolved investigations of proton-transfer dynamics. It is essentially protonated in the ground state in neutral aqueous solution, but excitation leads to rapid deprotonation.[11] Furthermore, its high charge (−3 for the acid, −4 for its conjugate base) creates a strong attraction between deprotonated HPTS and its dissociated proton, leading to significant diffusion-mediated recombination which can be leveraged to provide information on the nature of proton transport in different systems. MPTS, the methoxy derivative of HPTS, is also shown in Figure 1A. MPTS, which does not undergo excited-state proton transfer, is used as a probe of orientational dynamics because of its similarity to HPTS, and its time-dependent anisotropy can be measured without interference from excited-state deprotonation.

An important question in the study of processes in RMs and other confined aqueous environments is the impact of the nature of the interface. The influence of charged versus neutral surfactant−water interfaces on the dynamics of water molecules or dissolved probes in the water pools of RMs has been investigated by ultrafast visible[3] and infrared (IR)[3,7] spectroscopy and by NMR.[4]

Some previous investigations have been conducted on the dynamics of HPTS in ionic versus neutral RMs, using visible and IR pump−probe experiments.[3,4] These techniques are well-suited to examining the short-time behavior of HPTS but are generally limited in their ability to observe long-time dynamics, particularly the diffusion-mediated proton recombination with HPTS that takes place on nanosecond time scales. The time dependence of the recombination can be used to study the nature of the proton diffusion-like transport in various systems. The technique of time-correlated single-photon counting

Received: March 21, 2015
Revised: April 22, 2015
Published: April 26, 2015

DOI: 10.1021/acs.jpcb.5b02753
J. Phys. Chem. B 2015, 119, 6024−6034

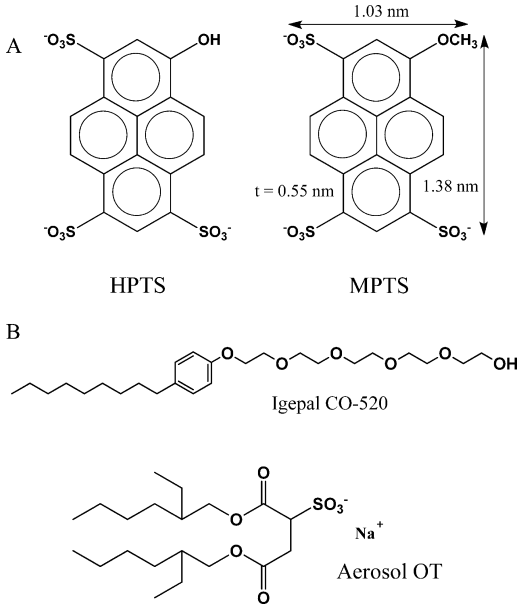

Figure 1. (A) Structures of photoacid HPTS and orientational relaxation probe, MPTS. The approximate dimensions of the molecules are shown. *t* is the thickness. (B) Structures of ionic and nonionic surfactants AOT and Igepal.

(TCSPC), used here to observe time-resolved fluorescence from HPTS and MPTS, is efficacious for observing these longer-time processes, as it can observe time scales from ∼100 ps to hundreds of nanoseconds. Previously, this approach was employed to investigate proton-transfer dynamics in ionic reverse micelles,[6] but it has not been applied to the study of proton transfer in nonionic RMs. In the studies presented below, the ionic RMs are composed of the surfactant Aerosol OT or more commonly AOT (sodium 1,4-bis[(2-ethylhexyl)-oxy]-1,4-dioxo-2-butanesulfonate). The neutral RMs are formed with the surfactant Igepal CO-520(polyoxyethylene (5) nonylphenylether), which will be termed Igepal. AOT has a sulfonate headgroup with a Na^+ counterion, whereas Igepal has a polyether chain with a terminal alcohol. Both surfactants are shown in Figure 1B. These two types of reverse micelles are well-characterized.[13−15] They are essentially monodispersed spheres with known sizes. By performing the experiments on nonionic RMs and comparing them to the same type of experiments on ionic RMs and bulk water, we aim to obtain a more complete picture of the influence of the environment on proton-transfer dynamics.

The results presented below display fundamentally different proton kinetics in neutral Igepal compared to that in ionic AOT. Fluorescence anisotropy measurements on MPTS show that it is located in the water nanopools AOT RMs, but it is associated with the surfactant−water interface in the Igepal RMs. The location of MPTS and HPTS in the RMs is determined by their intermolecular interactions with their environments in the ground electronic state. Both MPTS and HPTS consist of pyrene moieties and three sulfonates. As HPTS only differs from MPTS by having an alcohol rather than a methoxy, which will make a negligible change in the intermolecular interactions, HPTS will be located in the same regions of the two types of RMs. In AOT, the long-time scale population of the protonated state has a power law component to its decay that is independent of the RM size, with an exponent of −0.55 compared to the power law in bulk water, which new measurements presented here show has an exponent of −1.1. This exponent is close to the theoretically predicted exponent of −1.5.[16] The power laws are taken to be indicative of a diffusion-like process that moves the proton away from the deprotonated HPTS and thereby prevents recombination to the protonated state. In contrast, with HPTS bound to the wall of the Igepal RMs, there is no indication of power law kinetics. In Igepal, a kinetics model with no explicit diffusion accounts for the data and shows that the deprotonation time becomes shorter and the recombination time becomes longer as the size of the RMs becomes larger.

II. EXPERIMENTAL PROCEDURES

The surfactants AOT and Igepal CO-520 were purchased from Sigma-Aldrich and used as obtained. Stock solutions were prepared of 0.5 M AOT in *n*-heptane and of 0.3 M Igepal in a 50% w/w mixture of cyclohexane and *n*-hexane, and the water content of each stock solution was assessed by Karl Fischer titration. The size of the reverse micelles is determined by the molar ratio of the water concentration to the surfactant concentration.[14] This ratio is called w_0, and

$$w_o = \frac{[H_2O]}{[\text{surfactant}]} \quad (1)$$

The Igepal stock solutions were all found to have negligible water content, while the AOT stock solutions typically showed water content of $w_0 \sim 0.5$. This pre-existing water content was accounted for when preparing reverse micelles, which was done by adding the appropriate amount of water, containing the desired fluorescent probe, and shaking for a few seconds until all turbidity disappeared. The probe solutions used had a dye concentration of less than 1×10^{-5} M in all cases to avoid producing RMs with more than one probe molecule per micelle. For each surfactant, RMs of inner radii (water pool radii) 1.3, 1.6, 2.0, and 4.2 nm were prepared, which correspond to w_0 = 5, 7, 10, and 25 for AOT[14] and w_0 = 3, 5, 7, and 20 for Igepal.[17]

Time-resolved fluorescence data were obtained using the time-correlated single photon counting technique. The frequency-doubled output of a Spectra-Physics Mai Tai was used to excite samples with ∼100 fs pulses at a wavelength of 395 nm. A 1 mm thick sample cell was used to minimize the width of the instrument response, which was measured to be ∼50 ps. Single photons were detected with a Hamamatsu R3809U MCP photodetector and time-resolved with a Becker-Hickl SPC130 single-photon counting module.

For MPTS anisotropy measurements, fluorescence was collected with polarizations both parallel and perpendicular to the polarization of the excitation beam. This was achieved by rotating the polarization of the excitation beam with a half-wave plate in a computer-controlled rotation mount and setting the excitation polarization relative to a fixed analyzing polarizer mounted on the front of the monochromator.

Excited-state proton-transfer dynamics for HPTS in reverse micelles were investigated by measuring HPTS fluorescence with polarization at the magic angle (54.7°) relative to the polarization of the excitation beam. At this angle, orientational relaxation does not contribute to the time dependence of the fluorescence intensity, and the data yield the time-dependence of excited-state population.[18] Time-dependent fluorescence was measured across the emission spectrum from 410 to 530 nm in 2 nm increments.

DOI: 10.1021/acs.jpcb.5b02753
J. Phys. Chem. B 2015, 119, 6024−6034

Steady-state fluorescence spectra were collected with a Horiba Fluorolog FL3-221 fluorescence spectrometer. Samples were contained in 1 cm glass cuvettes, and spectra were acquired using right angle geometry.

III. RESULTS AND DISCUSSION

A. Anisotropy. The measured fluorescence intensities with polarization parallel ($I_{\parallel}(t)$) and perpendicular ($I_{\perp}(t)$) to the excitation source are related to the orientational correlation function of the probe molecule (second Legendre polynomial correlation function), $C_2(t)$, by

$$I_{\parallel}(t) = P(t)(1 + 0.8C_2(t)) \quad (2)$$

$$I_{\perp}(t) = P(t)(1 - 0.4C_2(t)) \quad (3)$$

where $P(t)$ is the population relaxation. The time-dependent anisotropy, $r(t)$, is obtained from $I_{\parallel}(t)$ and $I_{\perp}(t)$ as

$$r(t) = 0.4C_2(t) = \frac{I_{\parallel}(t) - I_{\perp}(t)}{I_{\parallel}(t) + 2I_{\perp}(t)} \quad (4)$$

The total anisotropy arises from orientational relaxation of the fluorescent probe molecule alone as well as from the rotation of the entire micelle.[1,2,19] These independent contributions can be separated according to

$$r(t) = 0.4C_p(t)C_m(t) \quad (5)$$

where $C_p(t)$ is the orientational correlation function for the probe only and $C_m(t)$ is the correlation function for the entire reverse micelle.

To isolate the rotation of the probe, the experimental time-dependent anisotropy is divided by the orientational correlation function for the entire micelle, calculated from theory assuming hydrodynamic rotation of the micelle, according to

$$C_m(t) = e^{-t/\tau_m} \quad (6)$$

$$\tau_m = \frac{\eta V}{k_B T} \quad (7)$$

where η is the dynamic viscosity of the solvent and V is the hydrodynamic volume of the micelle. Viscosities of *n*-heptane and 50/50 w/w cyclohexane/*n*-hexane were taken from the literature;[20,21] volumes of the reverse micelles were calculated by assuming spherical micelles and using literature values[13,17] for the dependence of the outer radii on w_0, corrected for the size of the MPTS molecule as in previous work[6] on AOT RMs. For all but the smallest reverse micelles, τ_m (given in Table 1) is so slow compared to the rotation of the probe molecule that it makes little difference.

Figure 2 shows the time-dependent anisotropy of MPTS in various reverse micelles, corrected for the rotation of the micelle, and in bulk water. Figure 2A shows data for AOT and exponential fits. The inset displays data on an expanded scale for both w_0 = 25 RM and bulk water with single exponential fits. The results for all of the RMs and bulk water are given in Table 1. In bulk water, the MPTS orientational relaxation is a single exponential with a time constant (τ_2) of 130 ps. In AOT w_0 = 25, the relaxation is also single exponential with a time constant (τ_2) of 150 ps. The virtual identity between the MPTS orientational relaxation time in bulk water and in AOT w_0 = 25 RMs demonstrates that the MPTS is located in the bulklike water core of the RMs. In larger reverse micelles, the water can be divided into two regions, the core and the shell.[5] The shell is composed of a thin layer of water molecules directly interacting with the interface. The core is the nanoscopic pool of water far enough removed from the interface that it behaves like bulk water.[5] The results also show that MPTS does not have an affinity for the interface and in fact tends to avoid the interface. If a significant fraction of the MPTS was associated with the interface, this subensemble would have a different orientational relaxation time, and a biexponential decay would be observed with one slow component and a bulk water component.

The MPTS orientational relaxation data in AOT w_0 = 10 RMs is a single exponential, but the orientational relaxation is about a factor of 2 slower than in bulk water. This result is

Table 1. Orientational Relaxation Parameters of Exponential Fits and Wobbling-in-a-Cone Angles for MPTS in AOT and Igepal Reverse Micelles and Bulk Water

sample	w_0	A_1[a]	τ_s (ns)	A_2[b]	τ_l (ns)	τ_w[c] (ns)	θ	τ_m[d] (ns)
bulk water	–	–	–	0.34	0.13	–	–	–
AOT	25	–	–	0.37	0.15	–	–	120
	10	–	–	0.31	0.32	–	–	32
	7	0.26	0.34	0.059	1.3	0.46	60°	22
	5	0.27	0.65	0.065	4.7	0.75	59°	17
Igepal	20	0.23	0.60	0.11	4.1	0.70	50°	150
	7	0.14	0.82	0.18	3.7	1.1	42°	29
	5	0.19	1.3	0.16	6.6	1.6	45°	21
	3	0.13	1.9	0.21	8.9	2.4	43°	14

[a] A_1 is the amplitude associated with the short time constant τ_s (where applicable). [b] A_2 is the amplitude associated with the long, complete reorientation time constant τ_l. [c] For samples that display wobbling-in-a-cone motion, τ_w is the wobbling time constant and θ is the cone half angle. [d] τ_m is the theoretically calculated time constant for reorientation of the entire micelle.

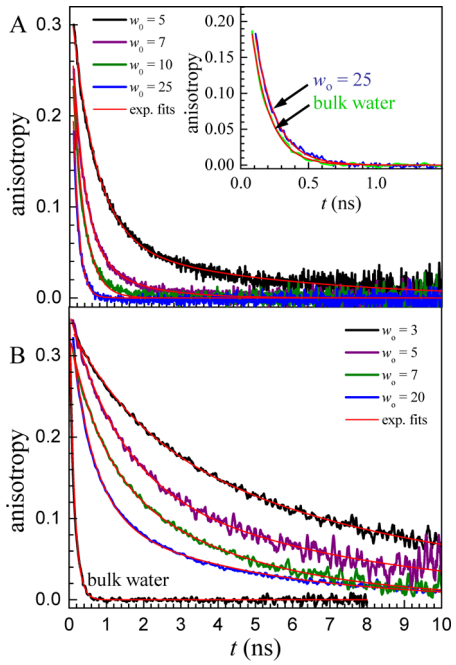

Figure 2. Time-dependent anisotropy decays of MPTS in AOT (A) and Igepal (B) RMs for various size water nanopools. The inset in panel A shows that the orientational relaxation in bulk water and the largest AOT RM are virtually identical. The red lines are single or biexponential fits to the data.

DOI: 10.1021/acs.jpcb.5b02753
J. Phys. Chem. B 2015, 119, 6024−6034

consistent with experiments on the nature of water in RMs as a function of size.[5] w_0 = 10 is the dividing line between large and small reverse micelles. Large RMs have a water core and a water shell at and near the interface. Small RMs ($<w_0$ = 10), are too small to have a core. The influence of the interface extends beyond the shell of water molecules in direct contact with the interface. In small reverse micelles, all of the water molecules in the nanopool are strongly affected by the interface. Ultrafast IR experiments that examine the water dynamics in reverse micelles[5] show that w_0 = 10 AOT RMs still have a core, but the water dynamics are slower than those in bulk water because the influence of the interface propagates out ~2 nm. Therefore, in w_0 = 10, MPTS is rotating free of direct interactions with the interface but in water that is not quite bulklike. Again, the single exponential decay shows that there is not a fraction of the MPTS directly interacting with the interface; therefore, in AOT, MPTS is likely repelled from the sulfonate head groups of AOT rather than attracted to them.

For the smaller AOT reverse micelles, w_0 = 5 and 7, there is a distinct change in the orientational relaxation dynamics. The decays are biexponential.[6] For these small RMs, there is no distinct water core. All of the water molecules are significantly affected by the interface. The water dynamics slow substantially.[5] In addition, the size of the small RMs makes interaction of the MPTS with the interface likely as the size of the water pool is approaching the size of the molecule.

The biexponential decay of MPTS anisotropy can be explained on the basis of restricted rotation of MPTS, which produces wobbling-in-a-cone behavior,[22−25] as has been reported for fluorescent probes in membranes[6,9,22,25] and some reverse micelles.[6,26] In this model, the probe undergoes relatively fast reorientation within a cone of half anlgle θ. Following the fast wobbling motion, complete orientational randomization can occur on a longer time scale. The result is a biexponential decay in which the fast component is the wobbling and the slow component is the final complete orientational relaxation. The orientational correlation function is represented by

$$C_p(t) = (S^2 + (1 - S^2)e^{-t/\tau_w})e^{-t/\tau_l} \quad (8)$$

where τ_w is the time constant for the restricted wobbling motion, τ_l the time constant for longer-time complete randomization, and S an order parameter related to θ by

$$S = \frac{1}{2}(\cos\theta)(1 + \cos\theta) \quad (9)$$

The longer time constant from the biexponential fit is τ_l, and τ_w can be calculated from τ_l and τ_s, the observed shorter time constant in the biexponential decay, by

$$\tau_w = (\tau_s^{-1} - \tau_l^{-1})^{-1} \quad (10)$$

The results of the fits are given in Table 1. The wobbling occurs in a cone with half angle of ~60°. For the small reverse micelles, the slow time constants for the complete orientational randomization are much slower than that of bulk water.

The results for AOT indicate that MPTS is not bound to the interface but rather is located in the water nanopool away from the interface. For the larger reverse micelles, the orientation relaxation is similar to that of MPTS in bulk water. For the smaller RMs, the restriction on water dynamics and the proximity of MPTS to the interface because of its size leads to restricted wobbling followed by complete relaxation. Because the only difference between MPTS and the photoacid HPTS is a methoxy versus a hydroxyl, HPTS should be situated in AOT reverse micelles as MPTS is.

The situation for MPTS in Igepal RMs is very different. Figure 2B shows the anisotropy data for MPTS in Igepal RMS with the same sizes as those used in the AOT experiments, although the w_0 values to achieve the same sizes differ for the two surfactants. Looking at Figure 2, it is clear that the anisotropy decays of MPTS in the Igepal RMs are much slower than in the AOT RMs. In addition, all of the data need a biexponential function to obtain a reasonable fit. Even the largest reverse Igepal RM displays a biexponential decay with the long time constant of 4.1 ns compared to 0.13 ns for bulk water and 0.15 ns for the AOT RM of the same size. Clearly something very different is occurring in the Igepal RMs compared to the AOT RMs.

The biexponential anisotropy decays of the MPTS in Igepal RMs were analyzed with the wobbling-in-a-cone model. The parameters are given in Table 1. Note that the parameters for the largest Igepal RM (water nanopool diameter, 8.4 nm) are almost the same as those for the smallest AOT RM (water nanopool diameter, 2.6 nm). The fact that even the largest Igepal RM gives rise to a biexponential decay and a very slow complete orientational relaxation time (τ_l, Table 1) indicates that for all sizes the MPTS is associated with the interface. The triply negatively charged MPTS may avoid the AOT interface, which is lined with negatively charged sulfonates. In contrast, the Igepal interface is composed of hydroxyls and ether groups, which will not have electrostatic repulsion for MPTS. As the Igepal RMs become smaller, both components of the biexponential decay become slower (see Table 1), demonstrating increasing restrictions on the motion that may occur from increasingly strong association of the MPTS with the interface. Despite being strongly associated with the interface, MPTS in Igepal RMs nevertheless retains significant orientational mobility, as evidenced by the fact that the slow reorientation times are still faster than the reorientation times of the entire micelle.

An alternative to the interface-associated wobbling-in-a-cone explanation for the biexponential orientational diffusion of MPTS in Igepal RMs might be a distribution of probe molecules between different environments, e.g., less-mobile probe molecules associated with the surfactant interface versus more freely rotating molecules in the core of the RM water pool. However, even the fast reorientation times for MPTS in Igepal RMs are significantly slower than the single reorientation times seen in AOT reverse micelles of the same size. This fact argues against the assignment of the two reorientation times in Igepal RMs to distinct interface-distributed and core-distributed populations of the probe and suggests instead that all of the MPTS molecules are surface-associated and thus experience slower orientational diffusion consistent with the wobbling-in-a-cone model.

The net result is that MPTS and, because of its virtually identical structure, HPTS are located in the water pools of AOT RMs away from the interface and only interact with the interface when the RM nanopool becomes very small. In contrast, in Igepal RMs, MPTS and HPTS are bound to the interface for all sizes of RMs and become increasingly tightly bound as the RM gets smaller. This difference in the location of HPTS in the two types of RMs has a major impact on the proton dynamics.

DOI: 10.1021/acs.jpcb.5b02753
J. Phys. Chem. B 2015, 119, 6024−6034

B. Proton Transfer. *1. Bulk Water.* In bulk water, the deprotonation of excited HPTS proceeds with a time constant of ~90 ps.[27] Despite this, significant protonated population exists even after several nanoseconds because of recombination of the dissociated proton with the deprotonated base. The rate of this recombination depends on proton transport in solution as well as on the kinetics of the back reaction itself. The conventional understanding of the excited-state proton transfer of HPTS and other photoacids in bulk water is that at long time ($t > 0.5-1$ ns[6,16]) and infinite dilution, the bound probability, $B(t)$, of the proton and photoacid (that is, the probability that the pair exists in the bound state) follows a $t^{-3/2}$ power law, according to the solution of the Debye−Smoluchowski equation for pairs with an electrostatic potential and back-reaction boundary conditions in a spherically symmetric three-dimensional space:[8,16]

$$B(t) \propto \frac{k_{eq}}{(4\pi Dt)^{3/2}} \tag{11}$$

where k_{eq} is the equilibrium constant for the reversible proton-transfer reaction and D is the combined diffusion constant for the proton and HPTS, which is overwhelmingly dominated by the diffusion of the much smaller proton. Thus, at long time the excited-state population, and therefore the fluorescence intensity, $I(t)$, of protonated HPTS in bulk water is taken to be a function of this power law recombination probability and the fluorescence lifetime, τ_f, of the fluorophore, according to

$$I(t) \propto e^{-t/\tau_f} t^{-n/2} \tag{12}$$

where n is the dimension of the system. For a three-dimension system, $n = 3$ and the power law exponent is $-3/2$.

Experimental verification of this long-time power law behavior is problematic;[28] the low intensity of the fluorescence from protonated HPTS at long time made good signal-to-noise and accurate background subtraction difficult to achieve. In particular, background subtraction is complicated because the blue wing of the fluorescence from deprotonated HPTS extends beneath the protonated emission peak. In bulk-water-like environments, in the long-time regime relevant to proton recombination dynamics, the deprotonated peak is so large relative to the protonated peak that even a small error in removing the contribution from the deprotonated fluorescence is significant.

The time dependence of the overlap of the protonated and deprotonated fluorescence spectra are shown in Figure 3, which displays the emission of HPTS in bulk water. In the analysis of proton transport in both bulk water and in the reverse micelles, it is necessary to know the fluorescence lifetimes of both the protonated and deprotonated species. For HPTS in bulk water, both lifetimes have been assigned as 5.4 ns.[29] The assignment that both lifetimes are the same can be tested by determining the integral of the entire spectrum as a function of time. The lower right inset in Figure 3 shows the time dependence of the integral of the spectrum and a single exponential fit, which yields 5.4 ns, showing that the two lifetimes are indeed the same. As discussed below, HPTS in AOT RMs also displays a single lifetime but HPTS in Igepal does not.

While the emission peaks for the protonated and deprotonated forms of HPTS, at 440 and 515 nm, respectively, are well-separated, within one nanosecond after excitation the amplitude of the protonated peak is more than an order of magnitude smaller than that of the deprotonated peak (see

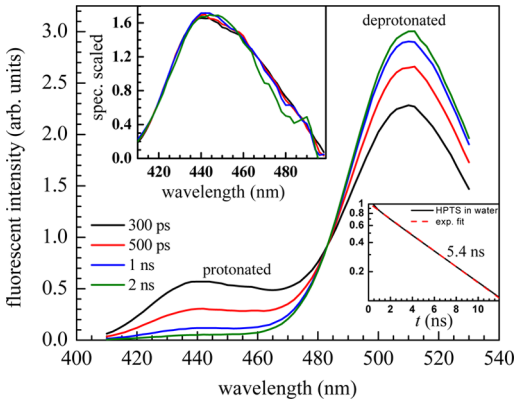

Figure 3. Time-resolved emission spectra of HPTS in bulk water. The integrals of the spectra as a function of time, shown in the inset, are the total excited-state population. The lower right inset shows that the total excited-state population decays as a single exponential. The upper left inset shows time-resolved emission spectra of protonated HPTS in bulk water after subtraction of the overlapping emission from the deprotonated form. The shape of the spectrum does not vary with time, demonstrating that it is the pure protonated emission, free from contamination from the deprotonated band.

Figure 3). The disparity in amplitude gives rise to a non-negligible contribution from the deprotonated species to the nominal protonated emission when the fluorescence is monitored at a single wavelength. This overlap of the spectra has previously been addressed experimentally by subtracting a time-dependent baseline from the measured fluorescence of the protonated form, with the parameters of the baseline either included as adjustable parameters in the fitting of the data or derived from the steady-state emission spectrum.[8,27] Here we use the entire spectrum. We use an accurate model of the deprotonated spectrum to perform the time-dependent baseline subtraction from the protonated fluorescence at each time point. By testing and then using this method, we achieve a rigorous subtraction of the deprotonated contribution to the protonated fluorescence and a reliable measure of the protonated fluorescence intensity as a function of time. In the upper left inset in Figure 3 we show the normalized, background-subtracted protonated peak for HPTS in bulk water at several time points. The consistent peak shape verifies that the background subtraction method is valid, i.e., if the shape of the deprotonated peak is incorrect, then as its amplitude increased with increased time, the shape of the protonated peak would change.

Figure 4 shows the time-dependent fluorescence intensity for protonated HPTS in bulk water (solid black curve). The fit to the data using the standard functional form given in eq 12 (dashed blue curve) is poor. In this fit, the power law exponent is fixed at −1.5 and the fluorescence lifetime, τ_f, is fixed at 5.4 ns (see Figure 3, lower right inset); only the amplitude is varied. Allowing the power law exponent to vary in the fit (red dashed curve), with the lifetime fixed at 5.4 ns, significantly improves the agreement. From 1 to 7 ns, the data has dropped from 10 000 to ~500. Over this time range, the fit almost perfectly reproduces the data, although there is still some deviation at longer times. In the fit in which the power law exponent is allowed to vary, there is an additional adjustable parameter. However, the Akaike statistical test[30] shows that the probability that the model with the fixed −1.5 exponent is a better model than that with the adjustable exponent is infinitesimally small. It

DOI: 10.1021/acs.jpcb.5b02753
J. Phys. Chem. B 2015, 119, 6024−6034

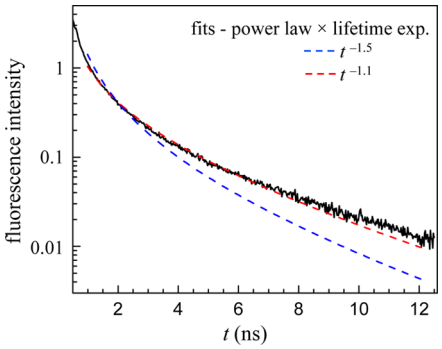

Figure 4. Time-dependent fluorescence intensity of protonated HPTS in bulk water (solid black curve). The blue dashed curve is the best fit to function $e^{-t/\tau_f}t^{-b}$ with b = 1.5, the theoretically predicted value and the measured fluorescence lifetime, τ_f = 5.4 ns (see Figure 3, lower right inset). Only the amplitude is allowed to vary. The red dashed curve is the fit with the power law exponent b and the amplitude allowed to vary. The best value for b is 1.1.

is important to note that the data were fit over a wide time range, from 1 to 12 ns.

There have been a number of studies that have reported a power law exponent of −1.5 for proton recombination with HPTS in bulk water.[6,8−10,27,31,32] There can be a number of reasons for the difference from the results shown in Figure 4. The data presented in Figure 4 has much better signal-to-noise ratio than much of the previously reported data, particularly relevant at long time. In addition, a more rigorous method for subtracting the contribution from a large deprotonated band was employed here. Furthermore, the time range of the data fit here is much larger than in many previous studies. Usually the data are multiplied by an increasing exponential, $\exp(t/\tau_f)$ to remove the lifetime contribution. The resulting curve is plotted on a log plot, and a region is selected that looks linear, typically between 1 and 3 ns. This region is compared to a line with a slope of −1.5. With an expectation of finding a slope of −1.5, adjusting the time-dependent baseline subtraction, and selecting a limited time range, it is possible to find the predicted exponent.

We are interested in the influence of nanoconfinement and the nature of the interface on proton transfer. We want the results on bulk water for comparison to the results obtained in the reverse micelles. Therefore, the reason that the bulk water exponent is −1.1 rather than the theoretical prediction of −1.5 will not be addressed in detail, but a few considerations might shed light on the matter. In the theoretical analysis,[16,27,33] the deprotonated HPTS is represented as a sphere with a negative four charge at its center. The proton is represented by a much smaller sphere with a positive 1 charge at its center. The spheres diffuse in a three-dimensional isotropic continuum. If the spheres touch, recombination can occur. However, deprotonated HPTS has four negative charges distributed around its perimeter (see Figure 1A). Three are on the sulfonates, and one is on the oxygen that gave rise to the proton following dissociation. In the actual sample, a proton that approaches and even contacts HPTS from the wrong direction cannot recombine. The proton must find the $-O^-$ that gave rise to it. A proton that leaves the immediate vicinity of the $-O^-$ and approaches the HPTS can be attracted to one of the negatively charged sulfonates. Because the sulfonates are so acidic, the proton will not bind, but this attraction can cause the proton to remain in the vicinity of the HPTS rather than recombining or permanently diffusing away. Subsequent diffusion around the HPTS may result in recombination to reform the protonated state. The attraction to the HPTS sulfonate negative charges may slow the loss of protons from neighborhood of the HPTS, giving rise to a reduction in the value of the exponent.

2. AOT Reverse Micelles. Figure 5 shows the time-dependent fluorescence intensity for the protonated form of HPTS in

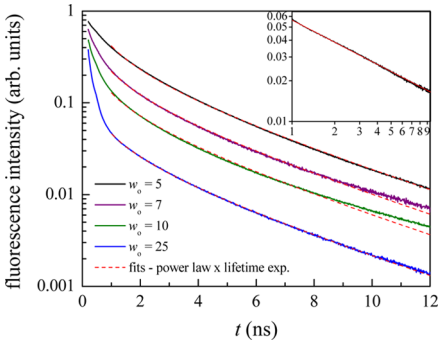

Figure 5. Time-dependent fluorescence intensity of protonated HPTS in AOT RMs (solid curves) and fits to $e^{-t/\tau_f}t^{-b}$, with τ_f fixed and b and the amplitude allowed to vary. The best value for b is 0.55.

AOT reverse micelles of various sizes (solid curves). We analyze this data using the same procedure as for bulk water, i.e., by fitting the data following the subtraction of the contribution from the deprotonated band using eq 12 but allowing the power law exponent to vary. Within experimental error (see Table 2) all of the power law exponents are the same,

Table 2. Long-Time Power Law Fits (t^{-b}) for HPTS in AOT Reverse Micelles

w_0	b
5	0.56 ± 0.03
7	0.56 ± 0.03
10	0.55 ± 0.03
25	0.55 ± 0.03

−0.55, that is, the power law is $t^{-0.55}$. This power law is in contrast to that found for bulk water, $t^{-1.1}$. In an earlier study, the AOT reverse micelle power law exponent was report as −0.8 for a variety of RM sizes and the bulk water exponent, −1.5.[6] As discussed above, the quality of the data and the data analysis presented here have been improved. The result is a reduction in both the bulk water and AOT RM exponents by about 25% from those reported previously.

In the largest AOT RM, w_0 = 25, the water pool is large enough that the central water core behaves like bulk water.[5] As discussed in section A, the orientational relaxation of MPTS in the w_0 = 25 AOT RM is virtually identical to that in bulk water (see Figure 3A inset). From the perspective of the HPTS, the various measurements show that the initial conditions for the proton dynamics in bulk water and the large AOT RM are essentially the same. Therefore, the difference in the power law exponents, −0.55 for AOT and −1.1 for bulk water, must come from the long time proton transport dynamics, that is, the manner in which the proton leaves the immediate vicinity of the HPTS, moves through the RM water nanopool, and ultimately recombines with the deprotonated HPTS to reform the protonated species. In contrast to bulk water, the proton

DOI: 10.1021/acs.jpcb.5b02753
J. Phys. Chem. B 2015, 119, 6024−6034

transfer is confined to a small, essentially spherical pool of water. AOT w_0 = 25 has a radius of 4.2 nm. HPTS has a radius of ~0.6 nm. Therefore, even in the largest RM, the HPTS is not far from the surfactant interface and the proton has a limited range of distances it can sample.

The fact that the −0.55 power law exponent is independent of size suggests that the difference in the power law exponent from that of bulk water is not simply due to confinement. If the AOT interface acted strictly as a reflecting boundary, one might expect the power law exponent to change as the size of the RM got smaller, although no analytical solution has been obtained for this problem in a finite spherical volume. In a spherical volume with no way for the proton to escape, it would be less likely for a proton to wander off and not recombine within the excited-state lifetime as the nanopool volume became smaller. In fact, there is a size effect, but not on the exponent. Figure 6

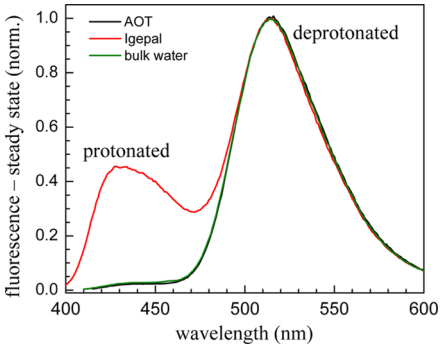

Figure 6. Steady-state emission spectra of HPTS in bulk water (green), w_0 = 25 AOT RMs (black), and w_0 = 20 Igepal RMs (red). The AOT and Igepal RMs have the same size water nanopools, r = 4.2 nm.

shows the normalized steady-state fluorescence spectra of HPTS in bulk water, AOT w_0 = 25, and Igepal w_0 = 20. The spectra for bulk water and AOT are very similar. There is a very small protonated band and a very large deprotonated band, but the ratios of the protonated peak to the deprotonated peak are somewhat different, that is, 0.028 for AOT w_0 = 25 and 0.023 for bulk water. Thus, there is an increase of ~20% in the protonated band amplitude in the RM. As the size of the RM decreases, the size of the protonated band relative to the deprotonated band increases. For the reverse micelle sizes, w_0 = 25, 10, 7, and 5, the ratios of the protonated band to the deprotonated band increases, with the ratios 0.03 ± 0.005, 0.06 ± 0.005, 0.09 ± 0.005, and 0.22 ± 0.005, respectively. As the size of the RM decreases, the probability of the HPTS being protonated increases substantially. This is consistent with the proton being confined in an increasingly small volume, which increases the rate of returns to the HPTS−O$^-$. The result is that the system spends a larger fraction of time in the protonated state.

The AOT−water interface is unlikely to be a pure reflecting boundary. It is possible that when the proton comes in contact with the interface it becomes trapped for some time and then is released back into the water pool. If there are a variety of types of "traps" such that some of them produced long-lived trapped species (comparable or long relative to the excited-state lifetime), then trapping could be the mechanism that prevents recombination. In bulk water, diffusion away from the deprotonated HPTS prevents recombination and is responsible for the power law decay. Here, diffusion in the water nanopool and long-lived trapping, which prevents recombination, could give rise to the observed power law.

3. Igepal Reverse Micelles. As discussed in section A, measurements of orientational relaxation show that HPTS is associated with the Igepal reverse micelle interface. This association is in contrast to HPTS in AOT RMs where the HPTS is located in the water pool away from the interface. For Igepal RMs, we anticipate that association of the photoacid and the surfactant−water interface will complicate the proton-transfer dynamics. A demonstration of the different nature of HPTS in Igepal RMs compared to bulk water or AOT RMs can be seen in the steady-state emission spectrum of HPTS, shown for bulk water and the largest Igepal and AOT RMs in Figure 6. As discussed above, the emission spectrum for the AOT reverse micelle is almost identical to the bulk water spectrum, with the steady-state deprotonated emission far larger than the protonated emission. In contrast, in the w_0 = 20 Igepal RMs, which have the same size water nanopool radius, ~4.2 nm, as the AOT w_0 = 25 RMs, the protonated peak is much larger. The larger protonated steady-state emission peak, which is time-averaged over the fluorescence lifetime, of Igepal relative to AOT indicates a significant difference in the proton-transfer dynamics. To understand the nature of this difference, it is necessary to see how the time-resolved emission spectrum evolves with time.

Figure 7 shows the time-resolved emission spectra for HPTS in Igepal w_0 = 20 RMs 200 ps, 1 ns, and 5 ns after excitation.

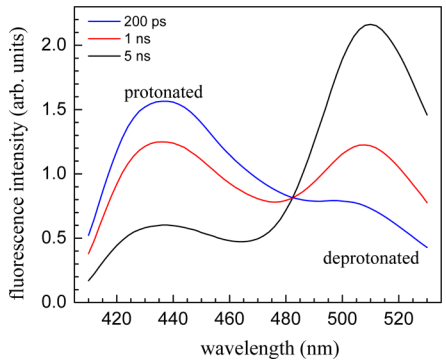

Figure 7. Time-dependent emission spectra of HPTS in w_0 = 20 Igepal RMs at 200 ps (blue), 1 ns (red), and 5 ns (black).

For both HPTS in water and in AOT reverse micelles, the time-dependent decays of the integrated area of the total spectra, protonated and deprotonated bands, were fit accurately with single exponentials, with a decay time of 5.4 ns in bulk water (see inset Figure 3) and 5.0 ns in AOT RMs. Those data show that in water and in AOT RMs, the protonated and deprotonated species have the same excited-state lifetimes and that there are not multiple species with different lifetimes. This is not the case for HPTS in Igepal RMs. Figure 8 shows the decay of the integrated spectrum of the excited state of HPTS in w_0 = 20 Igepal RMs (black solid curve) and a biexponential fit to the decay (dashed red curve) using

$$[\mathrm{HPTS}^*(t)] = A_1 e^{-t/\tau_{f1}} + A_2 e^{-t/\tau_{f2}} \quad (13)$$

The fit is essentially perfect. The inset shows the same data on a semilog plot (black solid curve) and a line drawn through the later potion of the data (dashed red line). Clearly the data are not single exponential, in contrast to the results for HPTS in water and AOT RMs (see lower right inset Figure 3). The

DOI: 10.1021/acs.jpcb.5b02753
J. Phys. Chem. B 2015, 119, 6024−6034

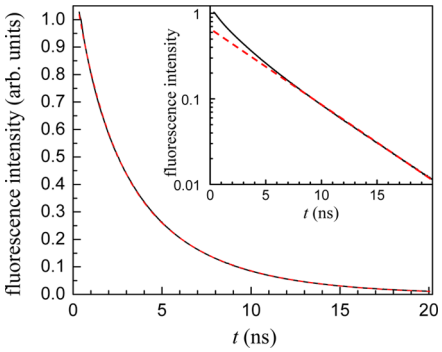

Figure 8. Total (protonated plus deprotonated) emission of HPTS in Igepal RMs, $w_0 = 20$ (solid black curve with a biexponential fit (dashed red curve). The inset shows the data on a semilog plot (solid black curve) and a line (dashed red line) clearly showing the nonexponential nature of the decay.

biexponential nature of the population decay indicates that there are two subensembles of HPTS molecules in Igepal RMs with distinct lifetimes. For $w_0 = 20$, the lifetimes are 1.8 and 5.0 ns.

The lifetimes for the various size Igepal RMs are given in Table 3. Both the longer lifetimes and the shorter lifetimes

Table 3. Lifetime and Proton-Transfer Fitting Parameters for HPTS in Igepal Reverse Micelles

w_0	A_1/A_2	τ_{f1} (ns)	τ_{f2} (ns)	τ_{dp} (ns)	τ_r (ns)
3	1.4	2.1 ± 0.1	5.4 ± 0.1	0.28 ± 0.04	0.39 ± 0.04
5	1.2	2.1 ± 0.1	5.2 ± 0.1	0.24 ± 0.02	0.66 ± 0.04
7	1.3	1.7 ± 0.1	5.1 ± 0.1	0.22 ± 0.02	0.60 ± 0.04
20	0.83	1.8 ± 0.1	5.0 ± 0.1	0.09 ± 0.02	1.2 ± 0.05

show a very mild trend of getting slightly faster as the RMs get bigger, but the differences are almost within the error bars. The longer-lived components are close to 5.4 ns, the lifetime of HPTS in bulk water.[29] Fluorescence lifetimes for HPTS shorter than those in water have been reported[34] in nonaqueous solvents, so a shorter lifetime component arising from interaction with the Igepal–water interface is plausible. This suggests that the HPTS molecules experience an environment that, while interface-associated as revealed by the MPTS anisotropy experiments, is also partially waterlike. This mixed environment may result from varying degrees of penetration of HPTS into the interfacial polyether region, or perhaps from a distribution of orientations, with HPTS sometimes "lying" relatively flat at the interface with greater polyether interaction and sometimes protruding more into the water pool, with consequently greater water interaction.

The time-dependent spectra in Figure 7 illustrate why single-wavelength measurements are inadequate for investigating the proton-transfer dynamics of HPTS in Igepal RMs. At short time, the protonated peak is larger than the deprotonated peak, while at long time the deprotonated peak is larger. There is considerable overlap between the two emission peaks over a broad time range, and the magnitude of the overlap changes substantially over the time scale of interest. Single-wavelength measurements of the fluorescence of the protonated and deprotonated forms will tend to include a significant time-dependent contribution from the fluorescence of the other form of HPTS. As can be seen in Figure 6, the spectrum of the deprotonated peak is identical in bulk water and in the two types of reverse micelles. As in the data analysis used for bulk water and AOT, a very accurate fit to the deprotonated peak is subtracted at each time point using the protonated band's amplitude at each time. The resulting protonated spectrum is free of contribution from the deprotonated band. To test the accuracy of the time dependence of the protonated data, we determined that the band shape did not change with time. In addition, obtaining the time dependence of the protonated species by using several different single wavelengths gave the same results.

Figure 9 displays the data for the time dependence of the protonated HPTS concentration for the four different size

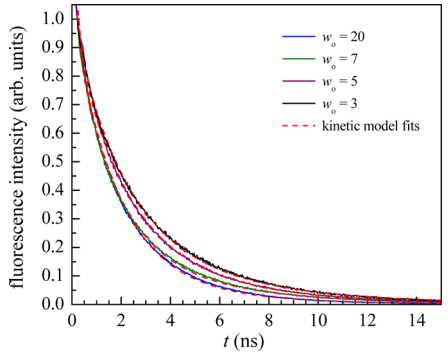

Figure 9. Time-dependent emission of protonated HPTS in Igepal RMs for various sizes (solid curves) and fits to the kinetic model (dashed red curves).

Igepal reverse micelles (solid curves). The protonated HPTS fluorescence in Igepal RMs cannot be fit to the functional form given in eq 12 even with n taken as a variable as was used to fit the bulk water data and the AOT RM data. In the absence of waterlike power law dynamics, we employ a kinetic model to analyze the proton-transfer dynamics and to account for the two subensembles of HPTS associated with the Igepal interface. The protonated and deprotonated excited populations for a single subensemble, $p(t)$ and $d(t)$, respectively, are given by

$$\frac{\mathrm{d}}{\mathrm{d}t}p(t) = \left(-\frac{1}{\tau_f} - \frac{1}{\tau_{dp}}\right)p(t) + \frac{1}{\tau_r}d(t) \quad (14)$$

$$\frac{\mathrm{d}}{\mathrm{d}t}d(t) = \left(-\frac{1}{\tau_f} - \frac{1}{\tau_r}\right)d(t) + \frac{1}{\tau_{dp}}p(t) \quad (15)$$

where τ_f, τ_{dp}, and τ_r are the time constants for fluorescence emission, deprotonation, and proton recombination, respectively. The proton recombination has been modeled as a first-order kinetic process. This model is sufficient to get good fits to the data, but a small nonexponential component to the recombination, which could be caused by some diffusive motion of the dissociated proton affecting the recombination rate, cannot be ruled out.

We allow the possibility of multiple distinct subensembles of HPTS molecules, each with its own τ_f, τ_{dp}, and τ_r. A good reproduction of the data is achieved with just two subensembles corresponding to the HPTS subensemble with the long lifetime and the HPTS subensemble with the short lifetime. While all of the HPTS in Igepal are associated with the surfactant interface, the long lifetime HPTS subensemble, with the lifetimes very similar to HPTS in bulk water (see Table 3), suggests that these HPTS have the hydroxyl group and much of the molecule

DOI: 10.1021/acs.jpcb.5b02753
J. Phys. Chem. B 2015, 119, 6024–6034

exposed to water (water-associated). The subensemble with the short lifetime most likely has the HPTS more buried in the surfactant interface with the hydroxyl not exposed to water (polyether-associated). For both subensembles, the negatively charged sulfonate groups will be exposed to water to solvate the charges. One possibility is that the water-associated HPTS are more or less lying flat on the surfactant surface, while the polyether-associated HPTS may have the portion of the molecule containing the hydroxyl (see Figure 1A) buried in the surfactant but leaving the sulfonates water-exposed.

In fitting the data in Figure 9 for each size RM, the relative populations (A_1/A_2) and the lifetimes (τ_{f1} and τ_{f2}) given in columns 2, 3, and 4 of Table 3, obtained from the analysis of the decay of the total excited-state population (see Figures 7 and 8), are fixed. Therefore, the fits involve only two adjustable parameters. The fits are the dashed red curves in Figure 9, and the results of the fits are given in the last two columns of Table 3. As can be seen in Figure 9, the fits are quite good for all four RM sizes.

The resulting fits demonstrate a lack of proton transfer in the polyether-associated subensemble, with deprotonation and recombination occurring only in the water-associated subensemble. The polyether-associated subensemble decays only via its excited-state lifetime. This is consistent with the picture in which hydroxyl is embedded in the surfactant wall and is not exposed to water. For the proton to dissociate, it needs to be solvated by water. For the water-associated HPTS, the deprotonation times obtained from the fits for the three small RMs are hundreds of picoseconds, longer than the 90 ps deprotonation time for HPTS in bulk water.[11] The deprotonation time becomes somewhat faster as the RM becomes larger. However, the largest RM, w_0 = 20, has the same deprotonation time as bulk water within experimental error. The three small RMs are considerably smaller than the largest w_0 = 20 RM (1.3, 1.6, and 2.0 nm, versus 4.2 nm). The surfactant−water interface surface areas and radii of curvature are much smaller for the three small RMs than for the largest RM. The differences in curvatures and surface areas will affect how HPTS associates with the interface and can result in HPTS in the large RMs having the hydroxyl more water exposed, resulting in faster deprotonation.

In bulk water, after the short time dynamics of the initial deprotonation, the time-dependent decay of the protonated species is caused by diffusion of the proton away from the parent HPTS. As the protons undergo diffusion, some of them will return to the HPTS and recombine to reform the protonated state followed by another round of deprotonation, and some of them will wander off into the bulk water. In addition, both the protonated and deprotonated forms decay to the ground state. The diffusion gives rise to the power law component of the decay, which is theoretically predicted to have an exponent of −1.5, with the experiments yielding an exponent of −1.1. In the water nanopools of AOT, the HPTS is not associated with the surfactant interface. Again a power law component of the decay is observed, but in the nanoconfined environment with the nearby surfactant−water interface, an exponent of −0.55 is obtained from fitting the data.

The model that successfully fits the proton dynamics in Igepal RMs differs from that for the other two systems. There is no clear reduction in the protonated species concentration arising from protons permanently diffusing away from the deprotonated HPTS, which would result in a power law component of the decay. The time constant τ_r is the recombination time. This model allows protons to recombine with deprotonated HPTS in its excited state to reform protonated HPTS in its excited state unless there is decay to the ground electronic state. The time constants for deprotonation and recombination, τ_{dp} and τ_r, respectively, as well as the excited-state lifetimes determine the population kinetics of the protonated and deprotonated HPTS species. As seen in Table 3, as the RM water nanopools become larger, the deprotonation time becomes faster and the recombination time becomes slower. As mentioned above, the reduction in the deprotonation time constant as the RM size increases may arise because the HPTS hydroxyl is increasingly water exposed. In addition, as the RMs become larger, the water hydrogen bond dynamics becomes faster,[5] increasing the ease of solvating the leaving proton. The slowing of the recombination as the RMs become larger may suggest greater ability of the proton to move some distance from the deprotonated HPTS prior to eventual recombination.

Another possible explanation for slower proton recombination in larger Igepal RMs could involve the changing structure of the surfactant interface. As the RMs become larger, the radius of curvature of the micelle increases, which changes the structure of the interface. In other types of RMs, it has been shown that changing the radius of curvature alters the headgroup area at the interface.[35,36] In Igepal RMs, the effective headgroup is not a simple ionic moiety as in AOT. The Igepal hydroxyl moiety (see Figure 1) has too little area to be the sole component of the headgroup. Rather, the headgroup is some combination of ethers and the hydroxyl. Altering the radius of curvature can change the chemical composition of the headgroup, for instance by exposing more ether units to the water interior. It is possible that the surfactant interface plays a role in determining the proton recombination rate, in which case the increasing radius of curvature and changing structure of the interface in larger RMs may affect this rate. For instance, the interface could contain proton "trapping" sites that prevent recombination until detrapping occurs. If so, the larger RMs might provide tighter or more numerous binding sites as a result of their different structures, requiring a longer average time to detrap and slowing recombination.

The Igepal proton-transfer model uses exactly two subensembles to represent the possible distribution of HPTS molecules. This is the minimum number required to reproduce the data. The two subensembles are consistent with the total excited-state population, protonated and deprotonated HPTS, decaying with two lifetimes. The model, which fits the data well, does not contain a reduction in recombination because protons leave the vicinity of the deprotonated species and do not return. We cannot rule out the possibility that some protons do diffuse away, but there is no evidence in the data, and the model without this possibility is sufficient to fit the data well (see Figure 9). HPTS in AOT RMs has proton-transfer dynamics very different than that of HPTS in bulk water, but both display power law decays indicative of protons leaving the deprotonated HPTS and not recombining. For Igepal RMs, HPTS is associated with the interface, which changes the fundamental nature of the proton recombination dynamics. For the Igepal surface bound HPTS, the experimental results demonstrate that all or at least the overwhelming majority of deprotonation events result in rapid recombination.

DOI: 10.1021/acs.jpcb.5b02753
J. Phys. Chem. B 2015, 119, 6024−6034

IV. CONCLUDING REMARKS

We have investigated the influence of nanoconfinement on proton-transfer dynamics in water following production of protons via excitation of a photoacid, HPTS. Of particular interest is the comparison between proton dynamics in the nanoscopic water pools of reverse micelles formed from a surfactant with ionic head groups (AOT) versus a neutral surfactant. The experiments are conducted on reverse micelles with a range of water nanopool sizes. In addition, the results are compared to those obtained for HPTS in bulk water. The nature of the interface, ionic versus neutral, results in major differences in the location of the photoacid and in the proton-transfer dynamics.

The orientational diffusion of the fluorescent probe MPTS and the excited-state proton-transfer dynamics of the fluorescent photoacid HPTS were studied by time-correlated single-photon counting. The time-dependent anisotropy of MPTS was found to be qualitatively different in the neutral Igepal RMs as opposed to the ionic AOT RMs. In the Igepal RMs, biexponential wobbling-in-a-cone reorientation dynamics were observed even in large water nanopools. In the AOT RMs, MPTS showed bulklike single exponential reorientation in the large micelles, with wobbling-in-a-cone behavior occurring only in the RMs with inner radii less than 2 nm, and even then the orientational relaxation is less restricted than the reorientation in Igepal RMs. These results show that MPTS and, because of its almost identical structure, HPTS are located in the central water core of the AOT RMs but are associated with the surfactant interface in the Igepal RMs.

Through improved signal-to-noise ratios and improved data analysis methodology, we have obtained very high-quality data on the time dependence of the protonated state of excited HPTS, free from artifacts that can be produced by the overlap of the deprotonated spectrum with the protonated spectrum. Theory has treated the proton as diffusing in a continuum with the photoacid and proton as spherical particles that undergo recombination following contact at any point.[16,27,33] The theory predicts a power law decay $t^{-1.5}$ of the protonated species population at longer times (> ~0.5 ns) for diffusion-controlled recombination of the proton with deprotonated HPTS. The power law arises from protons diffusing away from the deprotonated HPTS, not recombining, and therefore reducing the protonated state population. Our experimental results also yield a power law, but with a slower decay of $t^{-1.1}$ in contrast to previous experiments that faced lower signal-to-noise[6,8,10] and/or examined a more limited range of times.[32]

Enclosing the HPTS in the water nanopools of AOT reverse micelles has a profound effect on the proton recombination. A power law is still observed, but it is $t^{-0.55}$. The power law decay may still reflect the transport-induced reduction in recombination. The confinement in the water nanopools greatly reduces the rate of the transport-induced loss. The power law is independent of the size of the water nanopools, but as the RMs become smaller, the population of the protonated state under steady-state conditions increases.

The HPTS proton-transfer dynamics are fundamentally different in Igepal RMs compared to that in AOT RMs. HPTS is associated with the Igepal surfactant surface. There are two distinct subensembles as demonstrated by the biexponential decay of the total excited-state population, protonated plus deprotonated species. One of the subensembles has a shorter lifetime than HPTS in water and does not undergo proton dissociation to any experimentally detectable extent. This behavior is likely caused by the HPTS hydroxyl being buried in the organic wall of the RM. The other subensemble is taken to be on the surface with the hydroxyl water exposed. This subensemble does undergo deprotonation and recombination. However, the model with a power law component that describes transport-mediated recombination cannot describe the data. There is no evidence of a power law component to the decay, although if it was very small it might not be detectable in the data. A set of kinetic equations is used to analyze the data. Analysis of the data shows that as the water nanopool size increases the deprotonation time decreases and the recombination time increases. For the largest RM, the deprotonation time is the same as that found in bulk water.[11] The results show that the Igepal surface-bound and water-exposed HPTS undergo deprotonation, but the proton does not wander off into the water pools. These results may have broad implications for other types of systems in which a proton is generated at a water-exposed interface. Although water is available, the proton may remain associated with the interface.

AUTHOR INFORMATION

Corresponding Author

*E-mail: fayer@stanford.edu.

Notes

The authors declare no competing financial interest.

ACKNOWLEDGMENTS

We thank Joseph Thomaz for his aid with the experiments. This work was funded by the Division of Chemical Sciences, Geosciences, and Biosciences, Office of Basic Energy Sciences of the U.S. Department of Energy through Grant DE-FG03-84ER13251.

REFERENCES

(1) Wittouck, N.; Negri, R. M.; Ameloot, M.; De Schryver, F. C. AOT Reversed Micelles Investigated by Fluorescence Anisotropy of Cresyl Violet. *J. Am. Chem. Soc.* **1994**, *116*, 10601−10611.

(2) Visser, A. J. W. G.; Vos, K.; Van Hoek, A.; Santema, J. S. Time-Resolved Fluorescence Depolarization of Rhodamine B and (Octadecyl)Rhodamine B in Triton X-100 Micelles and Aerosol OT Reversed Micelles. *J. Phys. Chem.* **1988**, *92*, 759−765.

(3) Tielrooij, K. J.; Cox, M. J.; Bakker, H. J. Effect of Confinement on Proton-Transfer Reactions in Water Nanopools. *ChemPhysChem* **2009**, *10*, 245−251.

(4) Sedgwick, M.; Cole, R. L.; Rithner, C. D.; Crans, D. C.; Levinger, N. E. Correlating Proton Transfer Dynamics to Probe Location in Confined Environments. *J. Am. Chem. Soc.* **2012**, *134*, 11904−11907.

(5) Moilanen, D. E.; Fenn, E. E.; Wong, D.; Fayer, M. D. Water Dynamics in Large and Small Reverse Micelles: From Two Ensembles to Collective Behavior. *J. Chem. Phys.* **2009**, *131*, 014704.

(6) Spry, D. B.; Goun, A.; Glusac, K.; Moilanen, D. E.; Fayer, M. D. Proton Transport and the Water Environment in Nafion Fuel Cell Membranes and AOT Reverse Micelles. *J. Am. Chem. Soc.* **2007**, *129*, 8122−8130.

(7) Fenn, E. E.; Wong, D. B.; Fayer, M. D. Water Dynamics at Neutral and Ionic Interfaces. *Proc. Nat. Acad. Sci. U.S.A.* **2009**, *106*, 15243−15248.

(8) Huppert, D.; Goldberg, S. Y.; Masad, A.; Agmon, N. Experimental Determination of the Long-Time Behavior in Reversible Binary Chemical Reactions. *Phys. Rev. Lett.* **1992**, *68*, 3932−3935.

(9) Moilanen, D. E.; Spry, D. B.; Fayer, M. D. Water Dynamics and Proton Transfer in Nafion Fuel Cell Membranes. *Langmuir* **2008**, *24*, 3690−3698.

DOI: 10.1021/acs.jpcb.5b02753
J. Phys. Chem. B 2015, 119, 6024−6034

(10) Pavel, L.; Gepshtein, R.; Uritski, A.; Genosar, L.; Huppert, D. Effect of Electrolytes on the Excited-State Proton Transfer and Geminate Recombination. *J. Phys. Chem. A* **2006**, *110*, 5573−5584.
(11) Spry, D. B.; Goun, A.; Fayer, M. D. Deprotonation Dynamics and Stokes Shift of Pyranine (HPTS). *J. Phys. Chem. A* **2007**, *111*, 230−237.
(12) Pines, E.; Huppert, D. Observation of Geminate Recombination in Excited State Proton Transfer. *J. Chem. Phys.* **1986**, *84*, 3576−3577.
(13) Shukla, A.; Neubert, R. H. Investigation of W/O Microemulsion Droplets by Contrast Variation Light Scattering. *Pramana* **2005**, *65*, 1097−1108.
(14) Kinugasa, T.; Kondo, A.; Nishimura, S.; Miyauchi, Y.; Nishii, Y.; Watanabe, K.; Takeuchi, H. Estimation for Size of Reverse Micelles Formed by AOT and SDEHP Based on Viscosity Measurement. *Colloids Surf., A* **2002**, *204*, 193−199.
(15) Magid, L. J.; Daus, K. A.; Butler, P. D.; Quincy, R. B. Aggregation of Sulfosuccinate Surfactants in Water. *J. Phys. Chem.* **1983**, *87*, 5472−5478.
(16) Hong, K. M.; Noolandi, J. Solution of the Smoluchowski Equation with a Coulomb Potential. I. General Results. *J. Chem. Phys.* **1978**, *68*, 5163−5171.
(17) Lipgens, S.; Schubel, D.; Schlicht, L.; Spilgies, J.-H.; Ilgenfritz, G.; Eastoe, J.; Heenan, R. K. Percolation in Nonionic Water-in-Oil Microemulsion Systems: A Small Angle Neutron Scattering Study. *Langmuir* **1998**, *14*, 1041−1049.
(18) Lakowicz, J. R. *Principles of Fluorescence Spectroscopy*, 3rd ed.; Springer-Verlag: New York, 2008; Vol. *390*, pp 1223−1224.
(19) Szabo, A. Theory of Fluorescence Depolarization in Macromolecules and Membranes. *J. Chem. Phys.* **1984**, *81*, 150−167.
(20) Dymond, J. H.; Oye, H. A. Viscosity of Selected Liquid *n*-Alkanes. *J. Phys. Chem. Ref. Data* **1994**, *23*, 41−53.
(21) Wei, I. C.; Rowley, R. L. Binary Liquid Mixture Viscosities and Densities. *J. Chem. Eng. Data* **1984**, *29*, 332−335.
(22) Kinosita, K., Jr.; Kawato, S.; Ikegami, A. A Theory of Fluorescence Polarization Decay in Membranes. *Biophys. J.* **1977**, *20*, 289−305.
(23) Lipari, G.; Szabo, A. Model-Free Approach to the Interpretation of Nuclear Magnetic-Resonance Relaxation in Macromolecules. 1. Theory and Range of Validity. *J. Am. Chem. Soc.* **1982**, *104*, 4546−4559.
(24) Wang, C. C.; Pecora, R. Time-Correlation Functions for Restricted Rotational Diffusion. *J. Chem. Phys.* **1980**, *72*, 5333−5340.
(25) Lipari, G.; Szabo, A. Effect of Librational Motion on Fluorescence Depolarization and Nuclear Magnetic Resonance Relaxation in Macromolecules and Membranes. *Biophys. J.* **1980**, *30*, 489−506.
(26) Quitevis, E. L.; Marcus, A. H.; Fayer, M. D. Dynamics of Ionic Lipophilic Probes in Micelles: Picosecond Fluorescence Depolarization Measurements. *J. Phys. Chem.* **1993**, *97*, 5762−5769.
(27) Pines, E.; Huppert, D.; Agmon, N. Geminate Recombination in Excited State Proton Transfer Reactions: Numerical Solution of the Debye-Smoluchowski Equation with Backreaction and Comparison with Experimental Results. *J. Chem. Phys.* **1988**, *88*, 5620−5630.
(28) Solntsev, K. M.; Huppert, D.; Agmon, N. Challenge in Accurate Measurement of Fast Reversible Bimolecular Reaction. *J. Phys. Chem. A* **2001**, *105*, 5868−5876.
(29) Leiderman, P.; Genosar, L.; Huppert, D. Excited-State Proton Transfer: Indication of Three Steps in the Dissociation and Recombination Process. *J. Phys. Chem. A* **2005**, *109*, 5965−5977.
(30) Akaike, H. Information Theory and an Extension of the Maximum Likelihood Principle. In *2nd International Symposium on Information Theory*, Tsahkadsor, Armenia, USSR, September 2−8, 1971.
(31) Agmon, N.; Goldberg, S. Y.; Huppert, D. Salt Effect on Transient Proton Transfer to Solvent and Microscopic Proton Mobility. *J. Mol. Liq.* **1995**, *64*, 161−195.
(32) Agmon, N.; Pines, E.; Huppert, D. Geminate Recombination in Proton-Transfer Reactions. II. Comparison of Diffusional and Kinetic Schemes. *J. Chem. Phys.* **1988**, *88*, 5631−5638.
(33) Debye, P. Reaction Rates in Ionic Solutions. *Trans. Electrochem. Soc.* **1942**, *82*, 265−272.
(34) Htun, T. Excited-State Proton Transfer in Nonaqueous Solvent. *J. Fluoresc.* **2003**, *13*, 323−329.
(35) Eicke, H.-F.; Rehak, J. On the Formation of Water/Oil-Microemulsions. *Helv. Chim. Acta* **1976**, *59*, 2883−2891.
(36) Moilanen, D. E.; Fenn, E. E.; Wong, D. B.; Fayer, M. D. Geometry and Nanolength Scales Versus Interface Interactions: Water Dynamics in AOT Lamellar Structures and Reverse Micelles. *J. Am. Chem. Soc.* **2009**, *131*, 8318−8328.

DOI: 10.1021/acs.jpcb.5b02753
J. Phys. Chem. B 2015, 119, 6024−6034